Ultra-stable Silver Nanoparticles for Rapid Serology Detection of Anti-SARS-CoV-2 Immunoglobulins G

Journal:	*Analytical Chemistry*
Manuscript ID	ac-2022-00870b.R1
Manuscript Type:	Article
Date Submitted by the Author:	21-Apr-2022
Complete List of Authors:	Gosselin, Bryan; Universite Libre de Bruxelles, Service de Chimie Organique Retout, Maurice; Université libre de Bruxelles - Campus du Solbosch Dutour, Raphael; Université libre de Bruxelles - Campus du Solbosch Troian-Gautier, Ludovic; Université Libre de Bruxelles, Chemistry Bevernaegie, Robin; Universite Libre de Bruxelles, Service de Chimie Organique Herens, Sophie; Clinique CHC Monlégia Lefevre, Philippe; Vivalia Denis, Olivier; Sciensano Bruylants, Gilles; Universite Libre de Bruxelles, Engineering of Molecular NanoSystems, CP 165/64 Jabin, Ivan; Universite Libre de Bruxelles, Service de Chimie Organique

Ultra-stable Silver Nanoparticles for Rapid Serology

Detection of Anti-SARS-CoV-2 Immunoglobulins G

Bryan Gosselin, [a,b,#] Maurice Retout, [a,#] Raphaël Dutour, [a] Ludovic Troian-Gautier, [b] Robin Bevernaegie, [b] Sophie Herens, [c] Philippe Lefèvre, [d] Olivier Denis,[e] Gilles Bruylants [a,*] and Ivan Jabin [b,*]

[a] Engineering of Molecular NanoSystems, Ecole Polytechnique de Bruxelles, Université libre de Bruxelles (ULB), avenue F. D. Roosevelt 50, CP165/64, B-1050 Brussels, Belgium

[b] Laboratoire de Chimie Organique, Université libre de Bruxelles (ULB), Avenue F. D. Roosevelt 50, CP160/06, B-1050 Brussels, Belgium

[c] Service de Biologie Clinique, Clinique CHC Monlégia, Bvd Patience et Beaujonc 2, 4000 Liège, Belgium

[d] Service de Biologie Clinique, Hôpital de Marche groupe VIVALIA, Rue du Vivier 21, 6900 Marche en Famenne, Belgium

[e] Service Immune Response, Sciensano, Site Ukkel Engelandstraat 642, 1180 Brussels, Belgium

[*] Corresponding authors: Ivan.Jabin@ulb.be, Gilles.Bruylants@ulb.be

[#] These authors made equal contributions.

Graphical Abstract

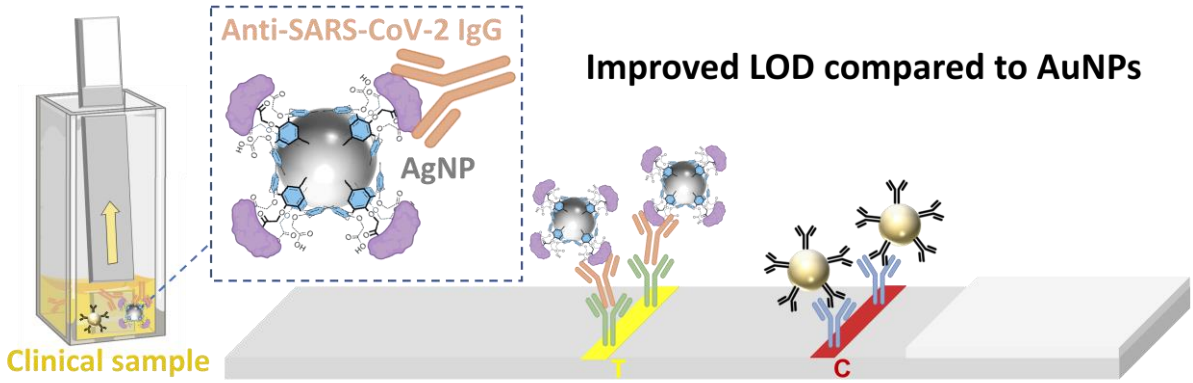

Abstract. Dipstick assays using silver nanoparticles (AgNPs) stabilized by a thin calix[4]arene-based coating were developed and used for the detection of Anti-SARS-CoV-2 IgG in clinical samples. The calixarene-based coating enabled the covalent bioconjugation of the SARS-CoV-2 Spike Protein via the classical EDC/sulfo-NHS procedure. It further conferred a remarkable stability to the resulting bioconjugated AgNPs, as no degradation was observed over several months. In comparison with Lateral-flow Immunoassays based on classical gold nanoparticles, our AgNPs-based system constitutes a clear step forward, as the limit of detection for Anti-SARS-CoV-2 IgG was reduced by one order of magnitude and similar signals were observed with 10 times less particles. In real clinical samples, the AgNPs-based dipstick assays showed impressive results: 100% specificity was observed for negative samples while a sensitivity of 73% was determined for positive samples. These values match the typical sensitivities obtained for reported LFIAs based on gold nanoparticles. These results i) represent one of the first example of the use of AgNPs-based dipstick assays in the case of real clinical samples, ii) demonstrate that ultra-stable calixarene-coated AgNPs could advantageously replace AuNPs in LFIAs and thus iii) open new perspectives in the field of rapid diagnostic tests.

Keywords: Silver Nanoparticles - Plasmonic Materials - Lateral Flow Immunoassays - SARS-CoV-2 - Rapid Diagnostic Test.

1. Introduction

The enzyme-linked immunosorbent assay (ELISA) is commonly used as a serological test for detecting proteins (e.g. biomarkers, antibodies). If ELISAs enable an accurate and sensitive detection, they however suffer from severe drawbacks including high production cost, long experiment time and the need for trained operators.[1] The COVID-19 crisis has shown that the development of alternative point-of-care (POC) methods allowing a convenient and rapid screening is urgently required.[2] Among all the rapid diagnostic tests (RDTs) developed over the past years, Lateral-flow Immunoassays (LFIAs) are probably the most widely used.[3-6] Indeed, LFIAs combine all the POC features such as simple read-out signal (naked eye observation), low cost and ease of use.[7]

Gold nanoparticles (AuNPs) are classically used as the colorimetric reporter in LFIAs because they exhibit a Localized Surface Plasmon Resonance (LSPR) band in the visible region and absorb light with an extinction coefficient higher by at least 3 orders of magnitude than any organic molecule.[8-9] In addition, their synthesis[10] as well as their surface modification with biomolecules[11-13] are well established. Nevertheless, if compared to ELISAs that often exhibit a limit of detection (LOD) in the nanomolar to picomolar range,[14] current AuNP-based LFIAs suffer from a poor sensitivity (LOD in the micromolar range). Recent efforts to improve the sensitivity of LFIAs have focused on signal amplification or on the use of a secondary signal obtained through fluorescence, surface-enhanced Raman spectroscopy or electrochemistry.[15-17] Unfortunately, most of these approaches require additional steps or supplementary equipment, which is not compatible with point-of-care testing.

To address this, we envisioned the use of a colorimetric reporter that would exhibit better optical properties than AuNPs, as it would not increase the assay time or its complexity. In this regard, silver nanoparticles (AgNPs) are plasmonic nanoparticles that also display a

LSPR band in the visible region but with an extinction coefficient one order of magnitude higher than the one of AuNPs of similar size. AgNPs could therefore lead to more sensitive LFIAs than AuNPs.[18] Their use has however been scarcely reported for the detection of proteins.[19-20] It is in part due to the weak chemical and colloidal stabilities of AgNPs in complex media or over time.[21] In contrast to AuNPs, AgNPs are indeed very sensitive to oxidation and their conjugation with biomolecules is thus difficult to achieve without important particles loss or degradation.[20-22] Moreover, their dispersion in biological fluids remains highly challenging.

Calix[4]arene-based coatings have recently been shown to improve drastically the colloidal stability of AgNPs as compared to commercially available ones.[23] These coatings are easily obtained via the irreversible reduction of calix[4]arene-tetradiazonium salts, leading to robust and thin organic monolayers (with typical thickness of *ca.* 2 nm).[24-26] In addition, we have shown that these ultra-stable AgNPs can be easily manipulated and conjugated to biomolecules such as proteins.[27] In this global pandemic context, we envisioned that calixarene-coated AgNPs could be advantageously used as colorimetric reporter in LFIA for the detection of Anti-SARS-CoV-2 immunoglobulins G (Anti-SARS-CoV-2 IgG). Up to now, more than 400 million people have been infected by SARS-CoV-2, causing more than 5.79 million reported deaths and making COVID-19 one of the worst plague of the 21st century (based on Johns Hopkins University data). Serological LFIAs using gold nanoparticles were rapidly and widely commercialized, as they enable the detection of IgM and IgG that are produced 3-6 days and 8 days after coronavirus infection, respectively.[28] Our hope was that AgNPs-based LFIAs would lead to a more reliable and efficient serological test with lower detection limits than AuNPs-based LFIAs.[1]

Herein we show with a dipstick design that calixarene-coated silver nanoparticles are valuable candidates for the development of LFIAs able to detect Anti-SARS-CoV-2 IgG in buffer, human plasma and real clinical samples.

2. Materials and methods

2.1. Chemical and biomolecules. All chemicals were at least reagent grade. Recombinant SARS-CoV-2 RBD Spike Protein were obtained from RayBiotech (230-30162) and Goat Anti-human IgG from Sigma-Aldrich (I2136). Fully human SARS-CoV-2 IgG were purchased from GeneTech. Blocker Casein Buffer (PBS) was obtained from Thermo Fisher and bovine serum albumin (BSA) >98 % from Sigma-Aldrich. Rabbit IgG (PP64) and Goat Anti-Rabbit IgG (SAB3700848) were obtained from Sigma-Aldrich. Commercial Prot A/G dipsticks were obtained from Abcam as part of "Check and go" conjugation kit. NC membranes were obtained from Cytiva for HP170 and Sartorius for CN140. Absorbent Pads SureWick (1.7x30 cm) were purchased from Sigma-Aldrich. The synthesis of the calix[4]arene-tetraacid tetradiazonium salt X_4 was achieved according to the literature[29] from commercially available *p*-*t*Bu-calix[4]arene (note however that the reduction of the nitro groups of the intermediate tetra-nitro derivative was achieved through hydrogenation (H_2, Pd/C) and not by using $SnCl_2$, as it was previously described). AuNPs-citrate with a mean core diameter between 15 and 20 nm were synthesized following a previously reported procedure.[30]

2.2. Characterizations and measurements. UV-Vis absorption spectra were recorded with a UV-Vis spectrophotometer in disposable semi-micro cuvettes (PMMA). As synthesized NPs were diluted by a factor of 10 in 1 mL aqueous solution, unless otherwise noted. Attenuated Total Reflection Fourier-transform Infrared (ATR-FTIR) spectra were recorded at 20°C on a FTIR spectrophotometer equipped with a liquid-nitrogen-cooled mercury−cadmium−telluride (MCT) detector. The silver nanoparticles were centrifugated and 2 µl of the pellet were deposited on a germanium internal reflection element (triangular prism of 6.8×45 mm^2 with an internal angle of incidence of 45°). Water was removed with a flow of nitrogen gas. Opus software (4.2.37) was used to record 128 scans with a resolution of 2 cm^{-1} under a continuous

flow of nitrogen gas over the sample. Data were processed and analysed using the Kinetics software in MatLab 7.1 (Mathworks Inc.,Natick, MA) by the subtraction of water vapour, baseline correction, apodization at 4 cm^{-1}, and flattening of the CO_2 signal. Finally, the spectra were normalized at 1459 cm^{-1} (aromatic ring stretching band from the calixarenes) to compensate for variations in the number of AgNPs present on the spot of the Ge crystal where the measurement was performed. Images of the AgNPs/AuNPs were obtained with a Transmission Electron Microscope (TEM) equipped with a lanthanum hexaboride (LaB6) crystal at a 200 kV accelerating voltage. The average size and standard deviation were determined by measuring the size of more than 150 NPs for each sample. Samples were characterized by dynamic light scattering (DLS) with back scattering (NIBS 173°). Measurements were performed at 25°C using a refractive index of 1.34 for the silver nanoparticles. AgNPs (5 µL~ 1 nM) were dispersed in lichrosolv water to obtain 1 mL of AgNPs (~0.05 nM) in disposable semimicro cuvettes (PMMA), and multiple DLS measurements were performed. The reported values are the average hydrodynamic diameter obtained from three independent measurements using the Z average as calculated by the Zetasizer software.

2.3. Synthesis of AgNPs-X_4. AgNPs-X_4 were synthesized following a previously reported procedure.[23] In a Protein-LoBind 50 mL-Falcon, 3 mL of $AgNO_3$ (10 mM) were mixed with 7.2 mL of an aqueous solution of calixarene X_4 (5 mM). 11.5 mL of lichrosolv water were then added. Finally, the pH was adjusted to 6.5 through the addition of the appropriate volume of 1M NaOH and, rapidly after this, 8.2 mL of sodium ascorbate were added. The resulting mixture was then heated at 60 °C and stirred at 1000 rpm using a thermomixer. After 16 hours of reaction, 60 µL of NaOH 1M were added in the tube. The Falcon was then centrifugated at 18,000 g for 20 minutes. The supernatant was discarded, and the particles were resuspended in a 5 mM NaOH solution. This washing cycle was repeated three times except that after the last

centrifugation the NPs were resuspended in MilliQ H_2O rather than in a 5 mM NaOH solution. The resulting AgNPs-X_4 were stored at room temperature.

2.4. Preparation of AgNPs-X_4-Prot-S or AgNPs-X_4-Goat IgG. In a 1.5 mL Protein Lobind Eppendorf, 500 µL of AgNP-X_4 (OD=6.2), 50 µL of MES buffer (100 mM, pH 5.8), 10 µL of 1-ethyl-3-(3-dimethylaminopropyl)carbodiimide chlorhydrate (EDC.HCl) (6 mM) and 10 µL of *N*-hydroxysulfosuccinimide (sulfo-NHS) (10 mM) were added successively. The activation step was carried out for 1 hour and the activated nanoparticles were centrifugated once (15 min., 15,000 g). The supernatant was discarded. The pellets were resuspended in MilliQ H_2O (500 µL) and then transferred in a 1.5 mL glass vial. Then, 50 µL of goat IgG (0.2 mg/mL) or 3 µL of SARS-CoV-2 recombinant protein (30 µM) were added and the reaction mixture was stirred for 4 hours at 1000 rpm at room temperature. 0.1 mL of 1% casein in 100 mM phosphate buffer (PB) pH 7.4 (with 150 mM NaCl) was added to the solution to block the AgNP surface. After incubation for 5 min at room temperature, the mixture was centrifuged at 15,000 g for 20 min. The supernatant was discarded and the AgNP conjugate was resuspended in 1.5 mL of 0.1% casein in 10 mM PB (with 15 mM NaCl). The centrifugation and resuspension cycle was repeated twice, and the final suspension solution was resuspended in 1X PBS. The resulting AgNPs-X_4-Prot-S or AgNPs-X_4-Goat IgG were stored at 4°C.

2.5. Preparation of AuNPs-citrate-Prot-S, AuNPs-citrate-Goat IgG or AuNPs-citrate-Rabbit IgG. 10 µL of SARS-CoV-2 recombinant protein (30 µM) or 20 µL of goat IgG (2 mg/mL) or 20 µL of rabbit IgG (2 mg/mL in 1X PBS) were added to a mixture of 1 mL AuNPs-citrate (OD=2) and 0.1 mL of borate buffer (0.1 M, pH 8.5). After incubation for 2h at room temperature, 0.1 mL of 1% casein in 100 mM phosphate buffer pH 7.4 (with 150 mM NaCl) was added to the solution to block the AuNP surface. After incubation for 15 min at room temperature, the mixture was centrifuged at 15,000 g for 20 min. The supernatant was discarded and the AuNP conjugate was resuspended in 1.5 mL of 0.1% casein in 10 mM phosphate buffer

pH 7.4 (with 15 mM NaCl). The centrifugation and resuspension cycle was repeated twice and the final suspension solution was resuspended in 400µL of 1X PBS. The resulting AuNPs-citrate-Prot-S, AuNPs-citrate-Goat IgG or AuNPs-citrate-Rabbit IgG were stored at 4°C.

2.6. Dipstick assembly. Anti-Rabbit IgG (2 mg/mL) were immobilized on the nitrocellulose membrane as the control line (C) and Goat Anti-Human IgG (2 mg/mL) were immobilized as the test line (T). The NC membrane was dried for 2 hours at 37°C and was then incubated for 10 minutes in the appropriate blocking buffer: 0.5% Casein or 1% BSA in water. After incubation, NC membranes were washed 5 times with MilliQ H_2O and dried at 37°C for 2 hours. Then, the absorbent pad was added on the NC membrane (with an overlap of 3 mm). Dipstick were cut into 5-mm strips and stored in a desiccator.

2.7. Dipstick assay procedure. In a disposable cuvette, 40 µL of running buffer (5% BSA, 0.2% Tween 20, 1% PEG-6000 in 0.5X PBS) and 10 µL of AgNP-X_4-Prot-S (OD=5) were mixed with 10 µL of plasma. After 15 minutes, the dipstick was partially immersed into the solution and read-out was performed after 15 minutes.

2.8. Sample collection. Serum samples were collected in the “Princesse Paola Hospital" of Marche-en-Famenne and in the "Sainte-Thérèse Hospital" of Bastogne from March 27 to May 4, 2020. Permission to conduct this study was obtained from the Ethics Committee of the VIVALIA Hospital group (study OM 152). Positive samples were obtained from adult patients tested positive for SARS-CoV-2 by PCR. A written informed consent was signed for all patients by patients themselves or by their legal representative if they were unable to give it. Control serums were collected in the beginning of January 2020 before the emergence of the SARS-CoV-2 in Belgium from a group of patients without any respiratory/infectious diseases.

2.9. ELISA procedure. Total and IgM antibodies specific for the receptor-binding domain of SARS-CoV-2 spike protein were analyzed using the Wantai SARS-CoV-2 Ab ELISA (Wantai

Biological Pharmacy, Beijing, China) (Wantai ELISA) following the manufacturer's recommendations. Results were calculated by relating each specimen absorbance value to the Cut-off value obtained from the absorbance of three negative calibrators. Results with a ratio greater than 1 are considered positive. Spike (S1/S2) specific IgG antibodies were analyzed using the LIAISON® SARS-CoV-2 IgG kit (DiaSorin S.p.A., Saluggia, Italy). This assay was performed on a LIAISON® XL Analyzer according to the manufacturer's instructions. The obtained results are quantitative and given as arbitrary units per milliliter (AU/mL). Values <12 AU/mL are considered negative.

3. Results and discussion

3.1. Preparation and characterization of calix[4]arene-coated silver nanoparticles. Readily available calix[4]arene-tetraacid tetradiazonium salt (X_4)[29] was deemed the ideal candidate for the development of dipstick devices as its four carboxyl groups can be covalently conjugated to proteins (**Figure 1A**). First, the corresponding calix[4]arene-coated silver nanoparticles (AgNPs-X_4) were obtained via the reduction of silver nitrate in the presence of calixarene X_4.[23] AgNPs-X_4 were then conjugated to the receptor binding domain (RBD) of the SARS-CoV-2 Spike Protein (Prot-S) via the classical EDC/sulfo-NHS procedure. After conjugation, the surface of the nanoparticles was blocked with casein to avoid further non-specific binding of endogenous proteins. The resulting nanoparticles AgNPs-X_4-Prot-S were thoroughly washed through several centrifugation/resuspension cycles and finally suspended in phosphate-buffered saline (1X PBS) solution.

The nanoparticles AgNPs-X_4 and AgNPs-X_4-Prot-S were characterized by UV-Vis and IR spectroscopies as well as by dynamic light scattering (DLS) and transmission electron microscopy (TEM). TEM analysis of AgNPs-X_4 revealed spherical monodisperse particles with a core size of 22 ± 3 nm (**Figure 1B**). AgNPs-X_4 exhibited a sharp and intense LSPR band with

a maximum (λ_{max}) centered at 417 nm, conferring to the suspension a bright yellow color (**Figure 1C**). The conjugation of Prot-S to the particles led to a 7 nm red-shift of λ_{max}, in agreement with the presence of a protein corona around the AgNPs-X_4-Prot-S (**Figure 1C**). No additional significant modification of the LSPR band could be observed, indicating that the silver nanoparticles did not aggregate during the conjugation process. Hydrodynamic diameters of approximately 35 nm and 67 nm were determined by DLS for AgNPs-X_4 and AgNPs-X_4-Prot-S, respectively (**Figure 1D**). These values are in good agreement with what was reported in the literature for the increase of the hydrodynamic diameter of AgNPs due to the adsorption of biomolecules.[19] AgNPs-X_4 as well as AgNPs-X_4-Prot-S (before the addition of casein in order to be able to distinguish the signals from the Prot-S) were characterized by FT-IR spectroscopy (**Figure 1E**). The typical bands corresponding to the calixarene structure[31] (*i.e.* at *ca.* 1450 and 1050 cm^{-1} for the aromatic ring stretching and the symmetric COC_{Ar} stretching, respectively) were visible on both types of NPs, indicating that the calixarene layer remained stable during the conjugation step. Moreover, intense amide I and II bands (at 1650 and 1530 cm^{-1}, respectively) were visible after bioconjugation, confirming the presence of Prot-S at the AgNPs surface.

Finally, the stability of AgNPs-X_4-Prot-S in non-diluted plasma was evaluated by UV-Vis spectroscopy. Strikingly, the thin calixarene-based coating conferred a remarkable stability to the functionalized NPs as no change of the LSPR band was observed over a period of one hour (Figure S1). This result highlights the fact that AgNPs-X_4-Prot-S are stable in complex media and opens the route to their use in real medical samples. It is worth noting that even in the absence of the protein corona, the particles (i.e. AgNPs-X_4) are stable in the presence of high salt concentration (1M NaCl) (Figure S2).

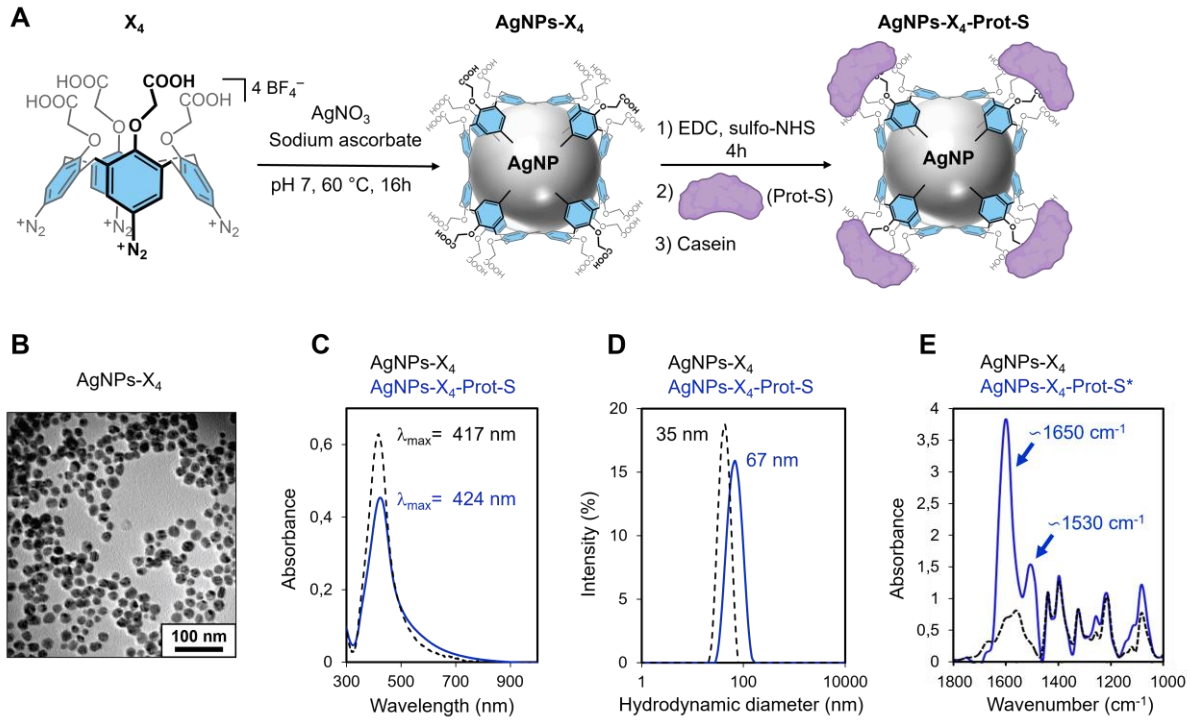

Figure 1. (A) Illustration of the synthesis of AgNPs-X_4-Prot-S. Note that the representation of the NP is schematic, as all calixarenes are not necessarily attached with four bonds to the surface and each Prot-S could be linked to multiple calixarenes. **(B)** TEM image of AgNPs-X_4. **(C)** UV-Vis spectra recorded in water at pH 7 for AgNPs-X4, before and after the coupling of Prot-S (AgNPs-X4-ProtS). **(D)** average hydrodynamic diameter obtained by DLS in water at pH 7. **(E)** IR spectra of AgNPs-X_4 (black dashed line) and AgNPs-X_4-Prot-S (blue plain line); *: before the addition of casein.

3.2. General principle of the dipstick assay for the detection of Anti-SARS-CoV-2 IgG.

Dipsticks composed of a nitrocellulose (NC) membrane and an absorbent pad were used for the development of the assay (**Scheme 1**). The test line (T) was coated with Anti-Human IgG and the control line (C) was coated with Anti-Rabbit IgG. AgNPs-X_4-Prot-S were used as the colorimetric reporter for the test line whereas rabbit IgG labelled AuNPs (AuNPs-citrate-Rabbit IgG, see the experimental part and Figure S3 for characterization) were used as the control colorimetric reporter. AgNPs-X_4-Prot-S were first incubated for 15 minutes with the plasma sample to form the SARS-CoV-2 antigen-antibody complexes. The dipstick was then immersed partially into the solution and this latter migrated entirely towards the absorbent pad in 15

minutes. In the presence of Anti-SARS-CoV-2 IgG in the plasma sample, the AgNPs-X4-ProtS-antibody complexes were captured by the IgG-binding proteins at the T line, generating a yellow-colored signal.

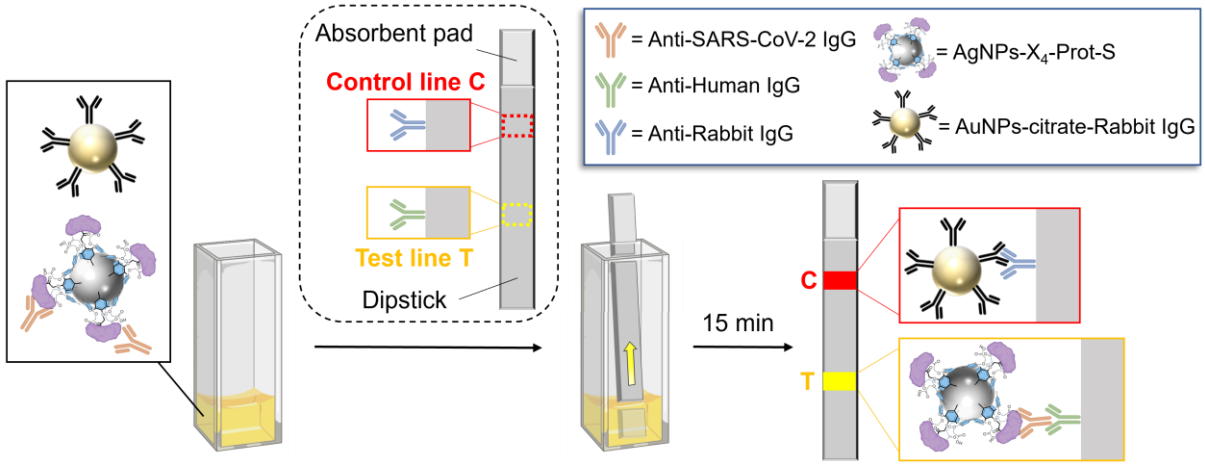

Scheme 1. Dipstick assay principle for the detection of Anti-SARS-CoV-2 IgG with calixarene-coated AgNPs. A mixture containing AgNPs-X4-Prot-S and AuNPs-citrate-Rabbit IgG is first incubated with a plasma sample containing Anti-SARS-CoV-2 IgG. After immersion of the dipstick and migration of the solution, the test line (T) and control line (C) are easily observed with the unaided eye as a yellow-colored line and a red-colored line, respectively.

3.3. Evaluation of silver nanoparticles as colorimetric reporter for dipstick assays. Before developing the AgNPs-based dipstick assay for Anti-SARS-CoV-2 IgG, we first determined the minimal amount of silver nanoparticles required to obtain a signal unambiguously observable with the naked eye. For this, we designed a simplified dipstick assay based on AgNPs-X_4 modified with goat IgG (*i.e.* AgNPs-X_4-goat IgG) and a commercial dipstick only displaying a T line coated with protein A (no C line). The high affinity of protein A for any IgG led to the immobilization of AgNPs-X_4-goat IgG and, as a result, to a yellow-colored T line that was observed at optical densities (OD) ranging from 0.4 to 0.01, which approximately corresponds to concentrations from 80 to 2 pM in AgNPs (**Figures 2a** and **2b**).

For comparison purposes, similar experiments were performed with citrate-capped gold nanoparticles (AuNPs-citrate), as these NPs are the reference material used in commercial LFIAs. AuNPs-citrate of 20 nm were synthesized and modified with goat IgG (see the experimental part and Figure S4 for characterization). In this case, the goat IgG was adsorbed on AuNPs-citrate, as these particles are not stable enough to endure the EDC/NHS coupling conditions. It is worth noting that various AuNPs allowing covalent conjugation of antibodies have been reported in the literature but commercial LFIAs are mostly based on AuNPs-citrate with adsorbed antibodies. The resulting AuNPs-citrate-goat IgG led, at optical densities of 0.4 and 0.1, to similar T line intensities than the corresponding AgNPs (**Figures 2a** and **2b**). For optical density of 0.01 or below, the signal of the silver nanoparticles was slightly more intense than the one of the AuNPs, probably because of the higher stability conferred by the calixarene coating. Despite a lower contrast of the yellow line obtained with AgNPs compared to the red one obtained with AuNPs on a white background, it is noteworthy that naked eye detection could be obtained with both sets of particles at similar OD. However, at same OD, ten times less AgNPs are used, as their molar extinction coefficient is approximately one order of magnitude larger than that of their Au counterparts. Less reporter nanoparticles means that less biomolecules are needed to prepare them and, consequently, a reduced production cost for the LFIA. In other words, these first results confirmed that AuNPs could be advantageously replaced by calixarene-coated AgNPs for the design of dipstick assays or LFIAs.

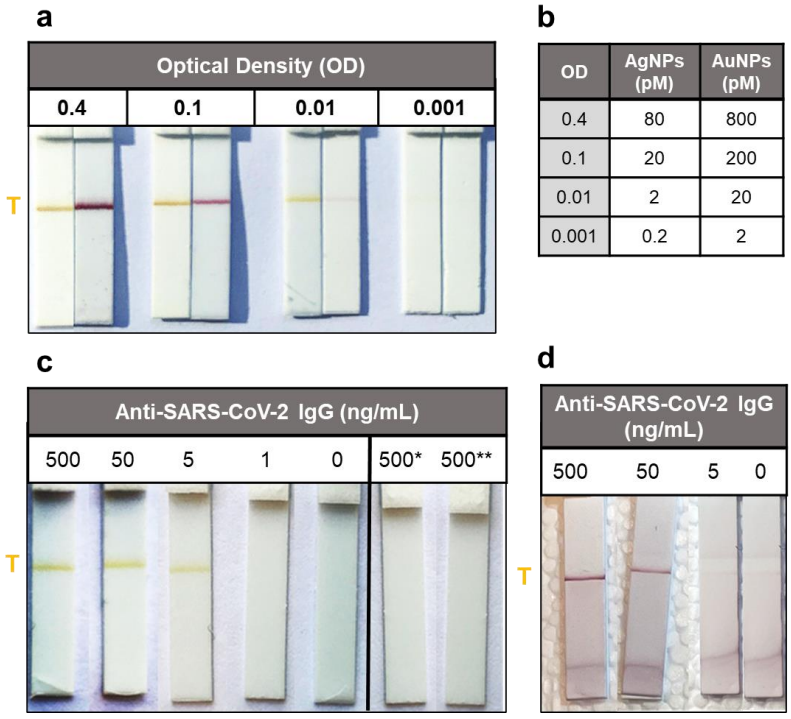

Figure 2. (a) Picture of the protein A dipstick incubated with decreasing concentrations of either AgNPs-X_4-goat IgG or AuNPs-citrate-goat IgG. (b) Concentration values of AgNPs-X_4-goat IgG and AuNPs-citrate-goat IgG for the different investigated optical densities (OD) in PBS. Pictures of dipsticks used to detect different concentrations of Anti-SARS-CoV-2 IgG with either (c) AgNPs-X_4-Prot-S or (d) AuNPs-citrate-Prot-S. Labels represent the concentration in ng/mL. *: 500 ng/mL of Anti-SARS-CoV-2 added to AgNPS-X_4. **: 500 ng/mL of goat IgG to AgNPs-X_4-Prot-S.

The detection of monoclonal Anti-SARS-CoV-2 IgG with AgNPs-X_4-Prot-S was then evaluated in PBS, using a similar simplified dipstick system (i.e. with a half-strip displaying only a T line coated with Protein A). AgNPs-X_4-Prot-S with OD = 0.1 were mixed with buffered solutions of Anti-SARS-CoV-2 IgG at concentrations ranging from 0 to 500 ng/mL. After 15 minutes of incubation, the dipsticks were immersed in the solution and, 15 minutes later, the T line was analyzed (**Figure 2c**). According to this procedure, a limit of detection (LOD) of 5 ng/mL was determined, which corresponds to an Anti-SARS-CoV-2 IgG concentration of *ca.* 33 pM. Replicates can be found in the Supporting Information as well as the detection of intermediate values (i.e., 20, 10 and 2 ng/mL) that confirm a LOD of 5 ng/mL (Figure S5). Note

that the visual observation results were confirmed through a quantification of the signal intensity using ImageJ software[32] (Figure S5D).

Control experiments showed the high selectivity of the calixarene-coated AgNPs system. Indeed, no colored T line was observed in the absence of Anti-SARS-CoV-2 IgG as well as upon the addition of (i) 500 ng/mL of Anti-SARS-CoV-2 IgG to unmodified AgNPs (*i.e.* AgNPs-X_4) or (ii) 500 ng/mL of goat IgG to AgNPs-X_4-Prot-S (**Figure 2c**). A comparison with the actual gold-standard material for LFIAs (i.e. AuNPs-citrate) with the protein-S adsorbed at its surface (*i.e.* AuNPs-citrate-Prot-S) was performed at similar ODs. A LOD of *ca.* 50 ng/mL was obtained with these particles (**Figure 2d**), as expected due to their inferior light extinction efficiency. Furthermore, a red trail was observed on all dipsticks, whatever the concentration of Anti-SARS-CoV-2 IgG investigated, which could lead to false positive errors. Taken together, these results show that i) the calixarene-coated AgNPs are particularly well-adapted to the design of efficient and highly sensitive LFIAs (with a sensitivity close to the one of traditional ELISAs) and ii) AgNPs-X4 are excellent colorimetric reporters for this type of system, as the LOD is reduced by one order of magnitude compared to classical AuNPs as a signal of at least similar intensity is obtained with 10 times less particles.

Finally, the detection of Anti-SARS-CoV-2 was performed with AgNPs-X_4-Prot-S stored at 4 °C for six months. The UV-Vis spectra of both freshly prepared and aged AgNPs-X_4-Prot-S were almost identical (**Figure 3**). Very interestingly, 6 months aged AgNPs-X_4-Prot-S remained capable of detecting 50 ng/mL of Anti-SARS-CoV-2 IgG in buffered solution with the same sensitivity and intensity than freshly prepared NPs (**Figure 3**, insets). This long shelf life of AgNPs-X_4-Prot-S can be explained by (i) the remarkably robust calixarene-based coating that strongly protects the AgNPs and (ii) the covalent immobilization of the Prot-S to the calixarene layer. This unique stability of calixarene-based AgNPs opens new perspectives in the field of RDTs, as particles shelf-life is a common issue for LFIAs.

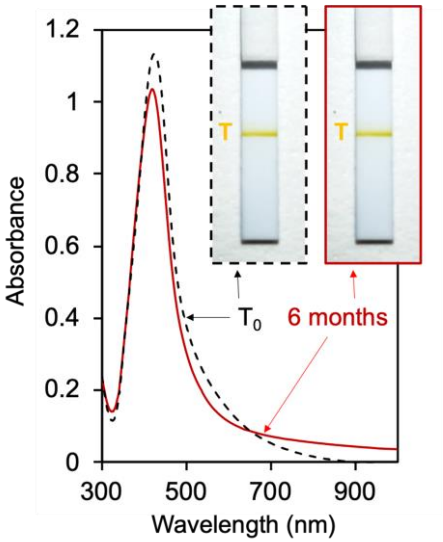

Figure 3. UV-Vis spectra of an AgNPs-X_4-Prot-S dispersion, as freshly prepared (black dashed line) and 6 months later (red plain line). Insets show the pictures of the dipstick used for the detection of 50 ng/mL of Anti-SARS-CoV-2 in PBS with either AgNPs-X_4-Prot-S freshly prepared (black dashed box) or 6 months later (red box).

3.4. Optimization of the Anti-SARS-CoV-2 IgG detection in a complex matrix. The serological testing for COVID-19 in biological fluids (e.g. blood, plasma or serum) is more complicated than in buffer solutions. Indeed, interferences between endogenous molecules and the AgNPs-Prot-S conjugates or with the proteins coating the dipstick could lead to a significant decrease of the signal intensity. As an example, the Protein A coated strips could not be used for the detection of Anti-SARS-CoV-2 IgG in spiked human plasma, as nearly no colored line could be observed even at high concentration (5 µg/mL) of Anti-SARS-CoV-2 IgG (Figure S6). It was thus necessary to optimize the dipstick assay to allow detection in human plasma. Parameters such as the composition of the dipstick, the type of membrane or the running buffer were screened. Best results were obtained when an intermediate-size pore CN140 membrane was used, and the test line was coated with goat Anti-human IgG (2 mg/ml) (Figures S7a-b). Moreover, it was shown that a blocking step of the membranes with a 0.5%wt casein buffer was crucial to avoid false positive results (Figure S7c). Finally, a running buffer containing

5%wt BSA, 0.2%wt Tween 20, 1%wt PEG 6000 and 0.5X PBS was determined as the most suitable (see Table S1 for details on running buffer screening).

The optimized dipstick assay was then used for the detection of monoclonal Anti-SARS-CoV-2 IgG spiked in human plasma as depicted in **Scheme 1**. For this, 10 µL of plasma were mixed with 10 µL of AgNPs-X_4-Prot-S (OD=5) dispersed in the running buffer. A yellow-colored T line was clearly observed until a concentration of Anti-SARS-CoV-2 IgG as low as 1.5 µg/mL (*i.e.* 10 nM) (**Figure 4a**). For lower concentrations, the intensity of the yellow line was too low to be detected unambiguously with the naked eye. The lower LOD obtained in plasma (1.5 µg/mL) compared to the one that was obtained in buffer (5 ng/mL) may be explained by the numerous immunoglobulins that can interact with the anti-human IgG immobilized on the T line and interfere with the immobilization of the particles. The experiments were repeated three times with three independent batches of AgNPs-X_4-Prot-S and the same LOD was determined by a panel of 5 observers (see Figure S8 for the pictures of the replicates). The signal intensity was also quantified using the ImageJ software,[32] confirming the LOD determined by visual observation (**Figure 4b**). It is worth mentioning that the median blood concentration of Anti-SARS-CoV-2 IgG is 16 µg/ml twenty days after the infection.[33] Similar experiments were performed with AuNPs-Prot-S and false positive results were obtained with plasma in the absence of Anti-SARS-CoV-2 IgG (Figure S9). This demonstrates the superiority of the AgNPs-X_4 as a colorimetric reporter for LFIAs. Also, it is worth noting that, 6-months aged AgNPs-X_4-Prot-S could still detect with the same sensitivity and intensity the Anti-SARS-CoV-2 IgG in human plasma (Figure S10).

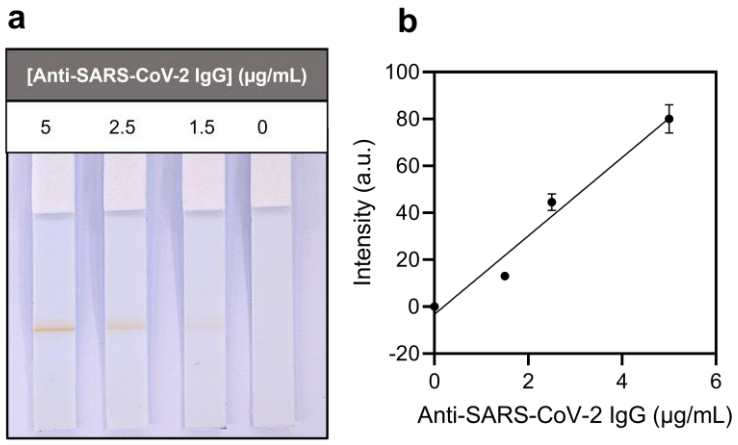

Figure 4. (a) Picture of the optimized dipstick assays used to detect different concentrations of monoclonal Anti-SARS-CoV-2 IgG spiked in human plasma. (b) Signal quantification from the pictures of the dipstick assays using ImageJ software ($R^2 = 0.965$). Note that the intensity values correspond to the average values of the three replicates.

3.5. Serological testing for Anti-SARS-CoV-2 IgG in real human samples. The detection conditions being optimized, the dipstick assay described in **Scheme 1** was used for the serological testing of Anti-SARS-CoV-2 IgG in 15 positive clinical samples (P1-15, confirmed by RT-PCR), obtained from SARS-CoV-2 infected patients, as well as in 10 negative samples (N1-10). The positive samples were first analyzed by Wantai Ig Total ELISA to sort them in three distinct groups of five samples (*i.e.* high, moderate and low Total Ig concentration groups), depending on their concentration in Anti-SARS-CoV-2 immunoglobulins (IgG, IgM, IgA, etc.). Furthermore, ELISA quantification of Anti-SARS-CoV-2 IgG was performed for all samples to better rationalize the results obtained from the dipstick assays (See Table S2 for ELISA titer value of all samples). Anti-Rabbit IgG were immobilized on the control line to bind AuNPs modified with Rabbit IgG (**Scheme 1**). This Rabbit /Anti-Rabbit IgG system was chosen at the C line to (i) avoid any cross-reactivity and (ii) to easily distinguish the red-colored C line from the yellow-colored T line thanks to the different plasmonic properties of AuNPs and AgNPs. All samples were analysed in duplicate, and the results were monitored independently by two operators.

The ten negative samples N1-10 were first tested, and no yellow T line was observed, indicating a 100% specificity of the AgNPs-X_4-Prot-S (**Figures 5b** and S11). The 15 PCR positive samples were then tested with our dipstick assay and 11 of them displayed a yellow band on the test line.

In the low concentrations Ig groups, 4 out of the 5 samples (P1-P4, Figure S12) displayed an IgG titer value below the cut-off level of ELISA (< 12 AU/mL). For samples P1 and P3-P4, the IgG titer values were however higher than the values measured for PCR negative samples. Interestingly, our lateral flow test presented a positive signal for these three samples, suggesting the detection of very small amounts of SARS-CoV-2 IgG, *i.e.* below the Elisa cut-off level. In the case of sample P2, the ELISA IgG titer value could not be distinguished from those obtained with PCR negative samples (< 3.8 AU/mL) which might explain why our dipstick assay was negative for that sample. Considering only the ELISA positive samples (titer above the threshold value), a yellow-colored test line was detected in eight (P5-P8, P10, P12, P14-15) out of the eleven positive samples (P5-15), which corresponds to a sensitivity of 73% (see **Figure 5a** for the moderate concentration Ig group and Figure S12 for the two other groups). The corresponding ELISA titers of Anti-SARS-CoV-2 IgG for the moderate Ig group are displayed in **Figure 5c**. Note that no correlation between signal intensities and ELISA titers was observed. It is worth mentioning that a sensitivity of 73% is also obtained if all PCR positive samples (P1-15) are considered, including those showing the lowest IgG titers.

The comparison of the results of the dipstick assays as function of PCR or ELISA analysis are summarized in **Figure 5d**. Regarding the ELISA positive samples, two of the three negative lateral flow tests belong to the high concentration Ig group (P11 and P13) and one to the moderate group (P9). Therefore, the absence of signal is not related to the limit of detection. A plausible explanation stems from the fact that other types of Ig (IgM, IgA) could bind to AgNPs-X_4-Prot-S or other types of IgG to the Anti-IgG line, respectively, interfering with and

limiting the immobilization of the particles on the test line. Nevertheless, these results are extremely promising. Indeed, they represent one of the first example of the use of a AgNPs-based dipstick assay in the case of real clinical samples.[34] Moreover, our system exhibits analytical performances that are similar to those of systems based on AuNPs (61-69 % sensitivity)[3-5] while using 10 times less particles to reach the same optical signal density (see Table S3 for some examples of commercial serological tests based on AuNPs and their sensitivity and specificity). Finally, we checked if our dipstick system could be used to design a real LFIA for the detection of Anti-SARS-CoV-2 IgG. To our delight, due to their high stability, the AgNPs-X_4-Prot-S could be dried on the conjugate pad and the resulting LFIA led to a similar detection performance than the dipstick assays (see the Supporting Information for the design of the LFIAs and Figure S13).

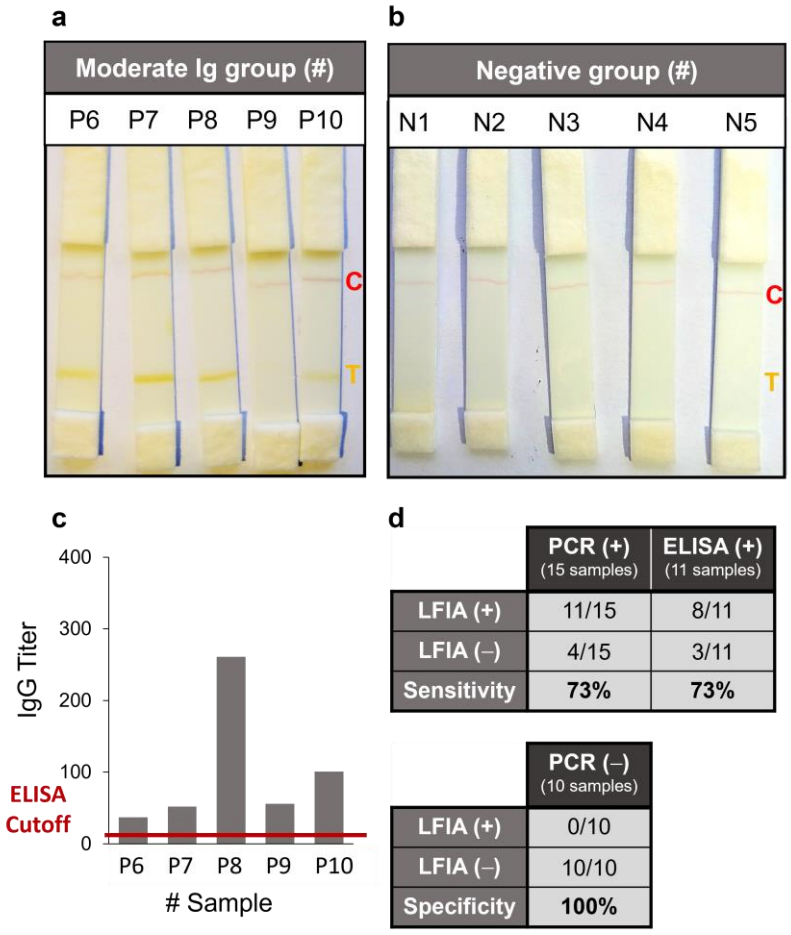

	PCR (+) (15 samples)	ELISA (+) (11 samples)
LFIA (+)	11/15	8/11
LFIA (–)	4/15	3/11
Sensitivity	**73%**	**73%**

	PCR (–) (10 samples)
LFIA (+)	0/10
LFIA (–)	10/10
Specificity	**100%**

Figure 5. Pictures of dipstick assays for (a) the moderate Ig concentration positive sample group and (b) negative samples. (c) Quantification of Anti-SARS-CoV-2 IgG by Wantai ELISA for moderate concentration Ig group. (d) Analytical performance table.

4. Conclusion

We have shown that ultra-stable silver nanoparticles coated by a thin layer of calix[4]arenes bearing carboxyl groups could be covalently conjugated with the SARS-CoV-2 Spike Protein (Prot-S) via the classical EDC/sulfo-NHS procedure. The resulting AgNPs-X_4-Prot-S are stable in complex matrixes such as human plasma and can be stored for months without any observable degradation, allowing their use for the development of LFIAs and the monitoring of real clinical samples. LOD of 5 ng/mL and 1.5 µg/mL were determined for the detection of Anti-SARS-CoV-2 IgG in buffer and in serum, respectively. These values are ten times lower than those obtained with traditional AuNPs-citrate despite the fact that ten times less AgNPs are used. These results suggest that the use of calixarene-coated AgNPs instead of AuNPs-citrate for the design of LFIAs could allow to improve the limit of detection as well as the operating cost while ensuring a long shell-live (more than six months) to the particles. Our AgNPs-based dipstick assay was used for the detection of SARS-CoV-2 IgG in clinical samples of patients tested positive (RT-PCR) for SARS-CoV-2 infection. A high specificity was obtained as no false positive was detected. Moreover, a sensitivity of 73% was determined, which corresponds to that of the traditional AuNPs-based LFIAs. All these results highlight the superior optical properties of AgNPs, compared to AuNPs, and the ultra-stability conferred by the calixarene coating to nanomaterials. These findings could benefit to anyone developing LFIAs, whatever the type of biomarker. Indeed, the high stability of the calixarene-based AgNPs and their conjugation capacity enable the covalent immobilization of a wide range of biomolecules such as proteins, antibodies, peptides, DNA aptamers, etc. Future work will be

directed toward the extension of our strategy to other types of silver nanomaterials in order to develop LFIAs displaying colored lines with a better contrast on a white substrate.

ASSOCIATED CONTENT

Supporting Information. UV-Vis and TEM characterization of AuNPs, detailed results about assay optimization, pictures of the dipstick assay for low and high Ig Tot group and ELISA titer tables of each clinical sample.

ACKNOWLEDGEMENTS

This research was supported by the Fonds pour la formation à la Recherche dans l'Industrie et dans l'Agriculture (FRIA-FRS) (PhD grant to B.G.), the Fonds de la Recherche Scientifique (FRS-FNRS) (postdoctoral grant to L.T.-G.), the "Actions de Recherches Concertées" of the Fédération Wallonie-Bruxelles and the ULB (PhD grant to M.R. and R.D.), the "Appel à projets Spécial COVID-19 - ULB", the Green Chemistry Program of Innoviris (postdoctoral grant to R.B.) and the "Fondation Jaumotte-Demoulin". We thank Dr. Vincent Lejeune (Hôpital de Marche, groupe VIVALIA) for his help in getting the clinical samples.

AUTHOR INFORMATION

Corresponding Authors

*E-mail: Ivan.Jabin@ulb.be, Gilles.Bruylants@ulb.be

Conflicts of interest

L. T.-G. and M. R. were postdoctoral researchers for X4C respectively from October 2014 to September 2015 and from August 2020 to January 2021. I. J. is a shareholder of X4C. I. J. and G.B. are consultants for X4C.

REFERENCES

(1) Liu, G.; Rusling, J. F. COVID-19 Antibody Tests and Their Limitations. *ACS Sens.* **2021**, *6* (3), 593–612. https://doi.org/10.1021/acssensors.0c02621.

(2) Song, Q.; Sun, X.; Dai, Z.; Gao, Y.; Gong, X.; Zhou, B.; Wu, J.; Wen, W. Point-of-Care Testing Detection Methods for COVID-19. *Lab Chip* **2021**, *21* (9), 1634–1660. https://doi.org/10.1039/D0LC01156H.

(3) Wen, T.; Huang, C.; Shi, F.-J.; Zeng, X.-Y.; Lu, T.; Ding, S.-N.; Jiao, Y.-J. Development of a Lateral Flow Immunoassay Strip for Rapid Detection of IgG Antibody against SARS-CoV-2 Virus. *Analyst* **2020**, *145* (15), 5345–5352. https://doi.org/10.1039/D0AN00629G.

(4) Huang, C.; Wen, T.; Shi, F.-J.; Zeng, X.-Y.; Jiao, Y.-J. Rapid Detection of IgM Antibodies against the SARS-CoV-2 Virus via Colloidal Gold Nanoparticle-Based Lateral-Flow Assay. *ACS Omega* **2020**, *5* (21), 12550–12556. https://doi.org/10.1021/acsomega.0c01554.

(5) Zeng, L.; Li, Y.; Liu, J.; Guo, L.; Wang, Z.; Xu, X.; Song, S.; Hao, C.; Liu, L.; Xin, M.; Xu, C. Rapid, Ultrasensitive and Highly Specific Biosensor for the Diagnosis of SARS-CoV-2 in Clinical Blood Samples. *Mater. Chem. Front.* **2020**, *4* (7), 2000–2005. https://doi.org/10.1039/D0QM00294A.

(6) Di Nardo, F.; Chiarello, M.; Cavalera, S.; Baggiani, C.; Anfossi, L. Ten Years of Lateral Flow Immunoassay Technique Applications: Trends, Challenges and Future Perspectives. *Sensors* **2021**, *21* (15), 5185. https://doi.org/10.3390/s21155185.

(7) Soh, J. H.; Chan, H.-M.; Ying, J. Y. Strategies for Developing Sensitive and Specific Nanoparticle-Based Lateral Flow Assays as Point-of-Care Diagnostic Device. *Nano Today* **2020**, *30*, 100831. https://doi.org/10.1016/j.nantod.2019.100831.

(8) Paramelle, D.; Sadovoy, A.; Gorelik, S.; Free, P.; Hobley, J.; Fernig, D. G. A Rapid Method to Estimate the Concentration of Citrate Capped Silver Nanoparticles from UV-Visible Light Spectra. *Analyst* **2014**, *139* (19), 4855. https://doi.org/10.1039/C4AN00978A.

(9) Liu, X.; Atwater, M.; Wang, J.; Huo, Q. Extinction Coefficient of Gold Nanoparticles with Different Sizes and Different Capping Ligands. *Colloids and Surfaces B: Biointerfaces* **2007**, *58* (1), 3–7. https://doi.org/10.1016/j.colsurfb.2006.08.005.

(10) Daruich De Souza, C.; Ribeiro Nogueira, B.; Rostelato, M. E. C. M. Review of the Methodologies Used in the Synthesis Gold Nanoparticles by Chemical Reduction. *Journal of Alloys and Compounds* **2019**, *798*, 714–740. https://doi.org/10.1016/j.jallcom.2019.05.153.

(11) Jazayeri, M. H.; Amani, H.; Pourfatollah, A. A.; Pazoki-Toroudi, H.; Sedighimoghaddam, B. Various Methods of Gold Nanoparticles (GNPs) Conjugation to Antibodies. *Sensing and Bio-Sensing Research* **2016**, *9*, 17–22. https://doi.org/10.1016/j.sbsr.2016.04.002.

(12) Retout, M.; Brunetti, E.; Valkenier, H.; Bruylants, G. Limits of Thiol Chemistry Revealed by Quantitative Analysis of Mixed Layers of Thiolated-PEG Ligands Grafted onto Gold Nanoparticles. *Journal of Colloid and Interface Science* **2019**, *557*, 807–815. https://doi.org/10.1016/j.jcis.2019.09.047.

(13) Biju, V. Chemical Modifications and Bioconjugate Reactions of Nanomaterials for Sensing, Imaging, Drug Delivery and Therapy. *Chem. Soc. Rev.* **2014**, *43* (3), 744–764. https://doi.org/10.1039/C3CS60273G.

(14) Liu, Y.; Zhan, L.; Qin, Z.; Sackrison, J.; Bischof, J. C. Ultrasensitive and Highly Specific Lateral Flow Assays for Point-of-Care Diagnosis. *ACS Nano* **2021**, *15* (3), 3593–3611. https://doi.org/10.1021/acsnano.0c10035.

(15) Xu, Y.; Liu, Y.; Wu, Y.; Xia, X.; Liao, Y.; Li, Q. Fluorescent Probe-Based Lateral Flow Assay for Multiplex Nucleic Acid Detection. *Anal. Chem.* **2014**, *86* (12), 5611–5614. https://doi.org/10.1021/ac5010458.

(16) Tran, V.; Walkenfort, B.; König, M.; Salehi, M.; Schlücker, S. Rapid, Quantitative, and Ultrasensitive Point-of-Care Testing: A Portable SERS Reader for Lateral Flow Assays in Clinical Chemistry. *Angew. Chem. Int. Ed.* **2019**, *58* (2), 442–446. https://doi.org/10.1002/anie.201810917.

(17) Bhardwaj, J.; Sharma, A.; Jang, J. Vertical Flow-Based Paper Immunosensor for Rapid Electrochemical and Colorimetric Detection of Influenza Virus Using a Different Pore Size Sample Pad. *Biosensors and Bioelectronics* **2019**, *126*, 36–43. https://doi.org/10.1016/j.bios.2018.10.008.

(18) Lee, J.-S.; Lytton-Jean, A. K. R.; Hurst, S. J.; Mirkin, C. A. Silver Nanoparticle−Oligonucleotide Conjugates Based on DNA with Triple Cyclic Disulfide Moieties. *Nano Lett.* **2007**, *7* (7), 2112–2115. https://doi.org/10.1021/nl071108g.

(19) Yen, C.-W.; de Puig, H.; Tam, J. O.; Gómez-Márquez, J.; Bosch, I.; Hamad-Schifferli, K.; Gehrke, L. Multicolored Silver Nanoparticles for Multiplexed Disease Diagnostics: Distinguishing Dengue, Yellow Fever, and Ebola Viruses. *Lab Chip* **2015**, *15* (7), 1638–1641. https://doi.org/10.1039/C5LC00055F.

(20) Anfossi, L.; Di Nardo, F.; Russo, A.; Cavalera, S.; Giovannoli, C.; Spano, G.; Baumgartner, S.; Lauter, K.; Baggiani, C. Silver and Gold Nanoparticles as Multi-Chromatic Lateral Flow Assay Probes for the Detection of Food Allergens. *Anal Bioanal Chem* **2019**, *411* (9), 1905–1913. https://doi.org/10.1007/s00216-018-1451-6.

(21) Pinzaru, I.; Coricovac, D.; Dehelean, C.; Moacă, E.-A.; Mioc, M.; Baderca, F.; Sizemore, I.; Brittle, S.; Marti, D.; Calina, C. D.; Tsatsakis, A. M.; Şoica, C. Stable PEG-Coated Silver Nanoparticles – A Comprehensive Toxicological Profile. *Food and Chemical Toxicology* **2018**, *111*, 546–556. https://doi.org/10.1016/j.fct.2017.11.051.

(22) Wang, Y.; van Asdonk, K.; Zijlstra, P. A Robust and General Approach to Quantitatively Conjugate Enzymes to Plasmonic Nanoparticles. *Langmuir* **2019**, *35* (41), 13356–13363. https://doi.org/10.1021/acs.langmuir.9b01879.

(23) Retout, M.; Jabin, I.; Bruylants, G. Synthesis of Ultrastable and Bioconjugable Ag, Au, and Bimetallic Ag_Au Nanoparticles Coated with Calix[4]Arenes. *ACS Omega* **2021**, *6* (30), 19675–19684. https://doi.org/10.1021/acsomega.1c02327.

(24) Mattiuzzi, A.; Jabin, I.; Mangeney, C.; Roux, C.; Reinaud, O.; Santos, L.; Bergamini, J.-F.; Hapiot, P.; Lagrost, C. Electrografting of Calix[4]Arenediazonium Salts to Form Versatile Robust Platforms for Spatially Controlled Surface Functionalization. *Nat Commun* **2012**, *3* (1), 1130. https://doi.org/10.1038/ncomms2121.

(25) Troian-Gautier, L.; Mattiuzzi, A.; Reinaud, O.; Lagrost, C.; Jabin, I. Use of Calixarenes Bearing Diazonium Groups for the Development of Robust Monolayers with Unique Tailored Properties. *Org. Biomol. Chem.* **2020**, *18* (19), 3624–3637. https://doi.org/10.1039/D0OB00070A.

(26) Li, D.; Luo, Y.; Onidas, D.; He, L.; Jin, M.; Gazeau, F.; Pinson, J.; Mangeney, C. Surface Functionalization of Nanomaterials by Aryl Diazonium Salts for Biomedical Sciences. *Advances in Colloid and Interface Science* **2021**, *294*, 102479. https://doi.org/10.1016/j.cis.2021.102479.

(27) Retout, M.; Gosselin, B.; Mattiuzzi, A.; Ternad, I.; Jabin, I.; Bruylants, G. Peptide-Conjugated Silver Nanoparticles for the Colorimetric Detection of the Oncoprotein Mdm2 in Human Serum. *ChemPlusChem* **2021**, cplu.202100450. https://doi.org/10.1002/cplu.202100450.

(28) Lee, H.-K.; Lee, B.-H.; Seok, S.-H.; Baek, M.-W.; Lee, H.-Y.; Kim, D.-J.; Na, Y.-R.; Noh, K.-J.; Park, S.-H.; Kumar, D. N.; Kariwa, H.; Nakauchi, M.; Heo, S.-J.; Park, J.-H. Production of Specific Antibodies against SARS-Coronavirus Nucleocapsid Protein without Cross Reactivity with Human Coronaviruses 229E and OC43. *J Vet Sci* **2010**, *11* (2), 165. https://doi.org/10.4142/jvs.2010.11.2.165.

(29) Troian-Gautier, L.; Valkenier, H.; Mattiuzzi, A.; Jabin, I.; den Brande, N. V.; Mele, B. V.; Hubert, J.; Reniers, F.; Bruylants, G.; Lagrost, C.; Leroux, Y. Extremely Robust and Post-Functionalizable Gold Nanoparticles Coated with Calix[4]Arenes via Metal–Carbon Bonds. *Chem. Commun.* **2016**, *52* (69), 10493–10496. https://doi.org/10.1039/C6CC04534K.

(30) Doyen, M.; Bartik, K.; Bruylants, G. UV–Vis and NMR Study of the Formation of Gold Nanoparticles by Citrate Reduction: Observation of Gold–Citrate Aggregates. *Journal*

of Colloid and Interface Science **2013**, *399*, 1–5. https://doi.org/10.1016/j.jcis.2013.02.040.

(31) Blond, P.; Bevernaegie, R.; Troian-Gautier, L.; Lagrost, C.; Hubert, J.; Reniers, F.; Raussens, V.; Jabin, I. Ready-to-Use Germanium Surfaces for the Development of FTIR-Based Biosensors for Proteins. *Langmuir* **2020**, *36* (40), 12068–12076. https://doi.org/10.1021/acs.langmuir.0c02681.

(32) Parolo, C.; Sena-Torralba, A.; Bergua, J. F.; Calucho, E.; Fuentes-Chust, C.; Hu, L.; Rivas, L.; Álvarez-Diduk, R.; Nguyen, E. P.; Cinti, S.; Quesada-González, D.; Merkoçi, A. Tutorial: Design and Fabrication of Nanoparticle-Based Lateral-Flow Immunoassays. *Nat Protoc* **2020**, *15* (12), 3788–3816. https://doi.org/10.1038/s41596-020-0357-x.

(33) Ma, H.; Zeng, W.; He, H.; Zhao, D.; Yang, Y.; Jiang, D.; Qi, P. Y.; He, W.; Zhao, C.; Yi, R.; Wang, X.; Wang, B.; Yang, Y. Y.; Kombe Kombe, A. J.; Ding, C.; Xie, J.; Gao, Y.; Cheng, L.; Li, Y.; Ma, X.; Jin, T. *COVID-19 Diagnosis and Study of Serum SARS-CoV-2 Specific IgA, IgM and IgG by Chemiluminescence Immunoanalysis*; preprint; Infectious Diseases (except HIV/AIDS), 2020. https://doi.org/10.1101/2020.04.17.20064907.

(34) Liu, H.; Dai, E.; Xiao, R.; Zhou, Z.; Zhang, M.; Bai, Z.; Shao, Y.; Qi, K.; Tu, J.; Wang, C.; Wang, S. Development of a SERS-Based Lateral Flow Immunoassay for Rapid and Ultra-Sensitive Detection of Anti-SARS-CoV-2 IgM/IgG in Clinical Samples. *Sensors and Actuators B: Chemical* **2021**, *329*, 129196. https://doi.org/10.1016/j.snb.2020.129196.